

RESEARCH

Open Access



# Impact of effective connectivity within the Papez circuit on episodic memory: moderation by perivascular space function

Ling-Ling Li<sup>1,2†</sup>, Jie Ma<sup>1†</sup>, Jia-Jia Wu<sup>1†</sup>, Xin Xue<sup>1</sup>, Mou-Xiong Zheng<sup>3\*</sup>, Xu-Yun Hua<sup>3\*</sup>, Qi-Hao Guo<sup>4\*</sup> and Jian-Guang Xu<sup>1,2,5\*</sup>

## Abstract

**Background and objectives** The formation and retrieval of episodic memory is dependent on the coordinated activity of multiple brain regions and neural networks, with the Papez circuit playing a critical role in this process. Recently, the role of the perivascular space (PVS) in cognitive function has garnered increasing attention. However, the role of PVS function between neural circuits and cognitive function in amnesic mild cognitive impairment (aMCI) patients remains unknown. Therefore, this study aims to (1) investigate alterations in the effective connectivity of the Papez circuit and PVS function in patients with aMCI and (2) explore the role of PVS function between the effective connectivity of the Papez circuit and episodic memory.

**Methods** Sixty participants, all of whom underwent multimodal MRI (fMRI, dMRI, and sMRI) and neuropsychological testing, were recruited for this case–control study. General linear models were used to compare the effective connectivity within the Papez circuit and PVS function between aMCI patients and healthy controls (HCs) and further explore the role of PVS function between the effective connectivity within the Papez circuit and episodic memory.

**Results** The effective connectivity between multiple critical regions within the Papez circuit, notably in the hippocampus, anterior cingulate cortex, and parahippocampal gyrus, was significantly weakened in aMCI patients. Moreover, a significant reduction in the along the perivascular space (ALPS) index was observed among aMCI patients, accompanied by a marked increase in PVS volume, indicating significant PVS dysfunction. Further moderation analysis revealed that PVS function moderated the relationship between effective connectivity within the Papez circuit and episodic memory.

<sup>†</sup>Ling-Ling Li, Jie Ma and Jia-Jia Wu contributed equally to this work.

\*Correspondence:  
Mou-Xiong Zheng  
zhengmouxiong@shutcm.edu.cn  
Xu-Yun Hua  
huaxuyun@shutcm.edu.cn  
Qi-Hao Guo  
qhguo@sjtu.edu.cn  
Jian-Guang Xu  
xjg@shutcm.edu.cn

Full list of author information is available at the end of the article



© The Author(s) 2025. **Open Access** This article is licensed under a Creative Commons Attribution-NonCommercial-NoDerivatives 4.0 International License, which permits any non-commercial use, sharing, distribution and reproduction in any medium or format, as long as you give appropriate credit to the original author(s) and the source, provide a link to the Creative Commons licence, and indicate if you modified the licensed material. You do not have permission under this licence to share adapted material derived from this article or parts of it. The images or other third party material in this article are included in the article's Creative Commons licence, unless indicated otherwise in a credit line to the material. If material is not included in the article's Creative Commons licence and your intended use is not permitted by statutory regulation or exceeds the permitted use, you will need to obtain permission directly from the copyright holder. To view a copy of this licence, visit <http://creativecommons.org/licenses/by-nc-nd/4.0/>.

**Conclusions** The effective connectivity within the Papez circuit and PVS function are closely related to cognitive function, particularly episodic memory, and enhancing PVS function may serve as a novel therapeutic target for slowing cognitive decline.

**Keywords** Perivascular space, Glymphatic system, Episodic memory, Moderation, Effective connectivity, Papez circuit, Multimodal MRI

## Introduction

Mild cognitive impairment (MCI) refers to a progressive decline in memory or other cognitive functions that does not significantly impact daily life and fails to meet the diagnostic criteria for dementia [1]. Amnesic mild cognitive impairment (aMCI), the most common subtype, is likely to progress to dementia, with an 80% probability of progressing within 6 years of diagnosis [2]. aMCI is characterized by significant episodic memory impairment, specifically difficulties in recalling the precise time and location of events [3]. Currently, neuroscientists are engaged in comprehensive investigations of the mechanisms and contributing factors of aMCI pathogenesis aimed at identifying strategies to address the barriers to cognitive rehabilitation in aMCI patients.

Considering that episodic memory depends on the coordinated activity of several specific regions and networks within the brain, the Papez circuit, which is a key neural network, plays a central role in this process [4]. The Papez circuit comprises the hippocampus (HPC), parahippocampal gyrus (PHG), anterior cingulate cortex (ACC), posterior cingulate cortex (PCC), and several other brain regions, which support episodic memory formation, consolidation, and retrieval via intricate interconnections [5]. For example, the HPC is essential for encoding and retrieving temporal and spatial details of specific events; the PHG supports contextual processing in episodic memory; and the cingulate cortex facilitates monitoring and regulating memory information [6]. Although the importance of the Papez circuit in episodic memory is widely recognized, certain limitations remain in current intervention studies on reversing memory decline in aMCI patients. In recent years, neuroscientists have explored methods to improve episodic memory in aMCI patients via neuromodulation techniques, including transcranial magnetic stimulation (TMS) and deep brain stimulation (DBS). However, while some studies have reported short-term improvements in memory performance, improvements in clinical efficacy compared with those of sham stimulation are small, with considerable individual variability [7, 8]. Some studies suggest that the limited efficacy may result from the stage of disease progression, differences in neural structures, and the progressive deterioration of neural network function in patients [9, 10]. On the basis of these findings, we hypothesize that the decline in episodic memory is not only caused by functional impairments in specific brain

regions but also involves more complex pathophysiological mechanisms, such as the glymphatic system (GS).

GS is not only the primary pathway for clearing metabolic waste in the brain but also plays a crucial role in maintaining the stability of the neuronal environment [11–13]. Studies indicate that GS facilitates efficient waste clearance through the circulation of cerebrospinal fluid (CSF) and interstitial fluid, thereby ensuring normal metabolic function in the brain [14–16]. Perivascular spaces (PVS), also known as Virchow–Robin spaces, are fluid-filled spaces that surround blood vessels within the brain [17]. A growing body of evidence suggests that PVS dysfunction may signal GS dysfunction, particularly in the early stages of neurodegenerative diseases [11, 18]. As the efficiency of this clearance mechanism declines, metabolic waste may accumulate between neurons, which can impair effective connectivity between them. Despite the potential link between PVS dysfunction and the Papez circuit, research in this field remains nascent and predominantly exploratory. Previous studies have calculated the time required for the brain to clear tracers after the intrathecal injection of contrast agents to reflect GS function, but the use of contrast agents poses risks of nephrotoxicity and potential neurotoxicity [19, 20]. Taoka introduced a noninvasive imaging technique to quantitatively assess PVS function—diffusion tensor imaging along the perivascular space (DTI-ALPS) [21]—which has demonstrated high repeatability, reliability, and consistency with gadolinium contrast-enhanced MRI following intrathecal injection [22]. Additionally, studies suggest that changes in PVS volume may be associated with changes in PVS function, thus providing an additional imaging marker for evaluating PVS function [23]. Studies have demonstrated that PVS dysfunction may serve as an early indicator of pathological changes in neurodegenerative diseases and could influence disease progression even before clinical symptoms manifest [24]. However, the role of PVS function between neural circuits and cognitive function remains unknown.

Therefore, this study aims to (1) investigate alterations in the effective connectivity of the Papez circuit and PVS function in patients with aMCI and (2) explore the role of PVS function between the effective connectivity of the Papez circuit and episodic memory. This study aims to provide novel insights into early diagnosis and intervention strategies for aMCI.

**Methods**

**Participants**

In this case-control study, we initially enrolled 106 participants from the Memory Clinic of Shanghai Jiao Tong University Affiliated Sixth People's Hospital and local communities in Shanghai from January 2020 to October 2023. Among them, 38 (35.85%) participants were excluded because they did not meet the eligibility criteria, 3 (2.83%) participants had incomplete neuropsychological testing, and 5 (4.72%) participants were excluded because they did not meet the image quality criteria. Finally, 28 (26.42%) aMCI patients and 32 (30.19%) healthy controls (HCs) matched for age, sex,

and education were included. Approval for the study was obtained from the ethics committee of Shanghai Jiao Tong University Affiliated Sixth People's Hospital (NO. 2019-041), in accordance with the Declaration of Helsinki, and all participants provided informed consent. The participant screening flowchart is presented in Fig. 1.

The inclusion criteria for the aMCI group included the following: (1) met Jak/Bondi's diagnostic criteria [25] (Supplemental Table S1); (2) had a Mini-Mental State Examination (MMSE) score greater than 24 points [26]; (3) were aged 55 to 80 years; (4) had objective memory impairment, with Auditory Verbal Learning Test Long-Term Delay Recall (AVLT-N5) and Recognition

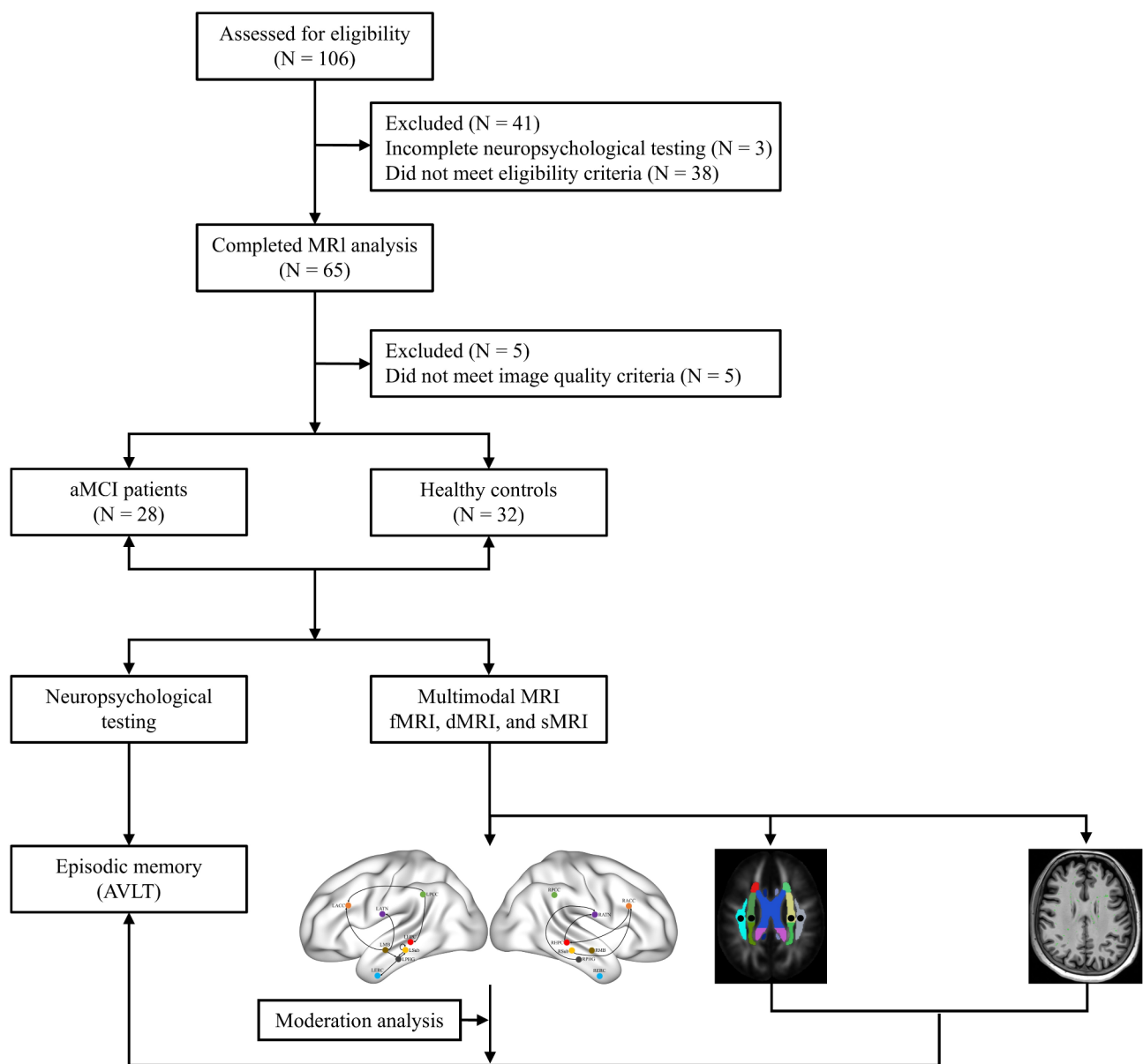


**Fig. 1** Flow chart of the study. aMCI, amnesic mild cognitive impairment; HCs, healthy controls; MRI, magnetic resonance imaging; fMRI, functional magnetic resonance imaging; dMRI, diffusion magnetic resonance imaging; sMRI, structural magnetic resonance imaging; AVLT, Auditory Verbal Learning Test

(AVLT-N7) scores falling below 1.0 standard deviation (SD) from the age-corrected normative mean [27]; (5) had complex Instrumental Activity of Daily Living (IADL) ability that might have been slightly impaired while still maintaining independent daily living [28]; (6) had a Clinical Dementia Rating (CDR) memory score of 0.5 [29] but did not meet the diagnostic criteria for dementia set by the National Institute on Aging-Alzheimer's Association (NIA-AA) [30]; and (7) were right-handed.

The exclusion criteria for all participants included the following: (1) a history of mental illnesses, including delirium, mania, depression, or anxiety; (2) contraindications for magnetic resonance imaging (MRI) examination; (3) less than 6 years of education; (4) severe aphasia and audio-visual impairment; (5) severe medical diseases, such as cardiopulmonary insufficiency, liver, or renal insufficiency; and (6) other diseases that cause cognitive impairment and white matter hyperintensity lesions, such as cerebrovascular disease, craniocerebral trauma, hydrocephalus, brain tumors, or intracranial infection.

### Neuropsychological testing

All participants underwent neuropsychological testing administered by two senior neuropsychologists who were blinded to the participants' clinical diagnoses. General cognitive function was assessed via the MMSE [26] and the Montreal Cognitive Assessment-Basic (MoCA-B) [31, 32]. Attention function was assessed via the Symbol Digit Modalities Test (SDMT) [33], and language function was assessed via the Boston Naming Test (BNT) [34]. Executive function was assessed via the Stroop test [35], and spatial function was assessed via the Judgment of Line Orientation (JLO) test [36]. Memory function was evaluated via the AVLT, and daily living activities were assessed via the Functional Activities Questionnaire (FAQ) [28].

### MRI acquisition

A 3.0 Tesla Magnetom Prisma scanner (Siemens Healthcare, Erlangen, Germany), which employs a head coil for scans ranging from the cranial vertex to the level of the foramen magnum, was used for the MRI scans. The MRI protocols included functional MRI (fMRI), diffusion MRI (dMRI), and structural MRI (sMRI). The participants were required to be free of recent colds and inflammation, maintain a quiet state for 30 min before the scan, and wear earplugs. During the scan, they were asked to lie still and quiet in the scanner, close their eyes without falling asleep, and try to keep their heads as still as possible. The detailed MRI protocols are provided in Supplemental Table S2.

### Data preprocessing

The standard pipeline of Statistical Parametric Mapping version 12 (SPM12, <https://www.fil.ion.ucl.ac.uk/spm/software/spm12/>) and the FMRIB Software Library (FSL, <https://fsl.fmrib.ox.ac.uk/fsl>, version 6.0.7) were used for fMRI data preprocessing. This data preprocessing pipeline included the exclusion of the first 10 volumes, slice timing correction, realignment, normalization, smoothing (6 mm full width at half maximum Gaussian kernel), detrending, ICA-based denoising (Automatic Removal of Motion Artifacts, AROMA) [37], regression covariates (Friston-24 head motion parameters and signals from white matter and cerebrospinal fluid) and filtering (0.01–0.08 Hz). Participants were excluded if they did not meet Satterthwaite's stringent framewise displacement (FD) criteria (including  $FD_{\text{Jenkinson}}$  and  $FD_{\text{Power}}$ ) [38, 39]. For sMRI data preprocessing, FSL was used to remove nonbrain tissue. Additionally, the recon-all pipeline from FreeSurfer (<https://surfer.nmr.mgh.harvard.edu/>, version 7.4.1) was utilized to obtain the total intracranial volume (TIV), which was used as a covariate in subsequent statistical analyses. Similarly, the standard pipeline of MRtrix3 (<https://www.mrtrix.org/>) [40] was used for dMRI preprocessing. This standard pipeline included denoising, Gibbs ringing removal, motion correction, eddy-current correction, top-up correction of susceptibility distortions, and bias field correction. Meticulous data quality checks were performed during preprocessing and all subsequent processing steps to ensure the images' integrity and precision.

### Effective connectivity within the Papez circuit

Effective connectivity analysis includes the following steps (Fig. 2A): (1) Extraction of the time series of all brain regions in the Papez circuit. The model was constructed by placing spheres (radius = 6 mm) in the following regions of interest (ROIs): the left and right anterior thalamic nuclei (ATN, MNI coordinates:  $\pm 4 - 1 0$ ), the left and right entorhinal cortex (ERC, MNI coordinates:  $\pm 26 - 1 - 33$ ), the left and right mamillary body (MB, MNI coordinates:  $\pm 2 - 7 - 14$ ), and the left and right subiculum (Sub, MNI coordinates:  $\pm 27 - 18 - 16$ ) [41]. For the left and right ACC, HPC, PCC, and PHG, bilateral masks of these regions were constructed via the WFU PickAtlas toolbox (<http://fmri.wfubmc.edu/software/PickAtlas>) [41]; (2) For each participant, a fully connected model of the left and right Papez circuit was established, and spDCM was used for the parameter estimation of the fully connected model [42, 43]; (3) The group-level connectivity parameters were estimated via the parametric empirical Bayes (PEB) algorithm, and the effective connectivity parameters of the group model obtained via the Bayesian model averaging (BMA) algorithm were averaged to derive the group-level effective connectivity strength [42, 43].

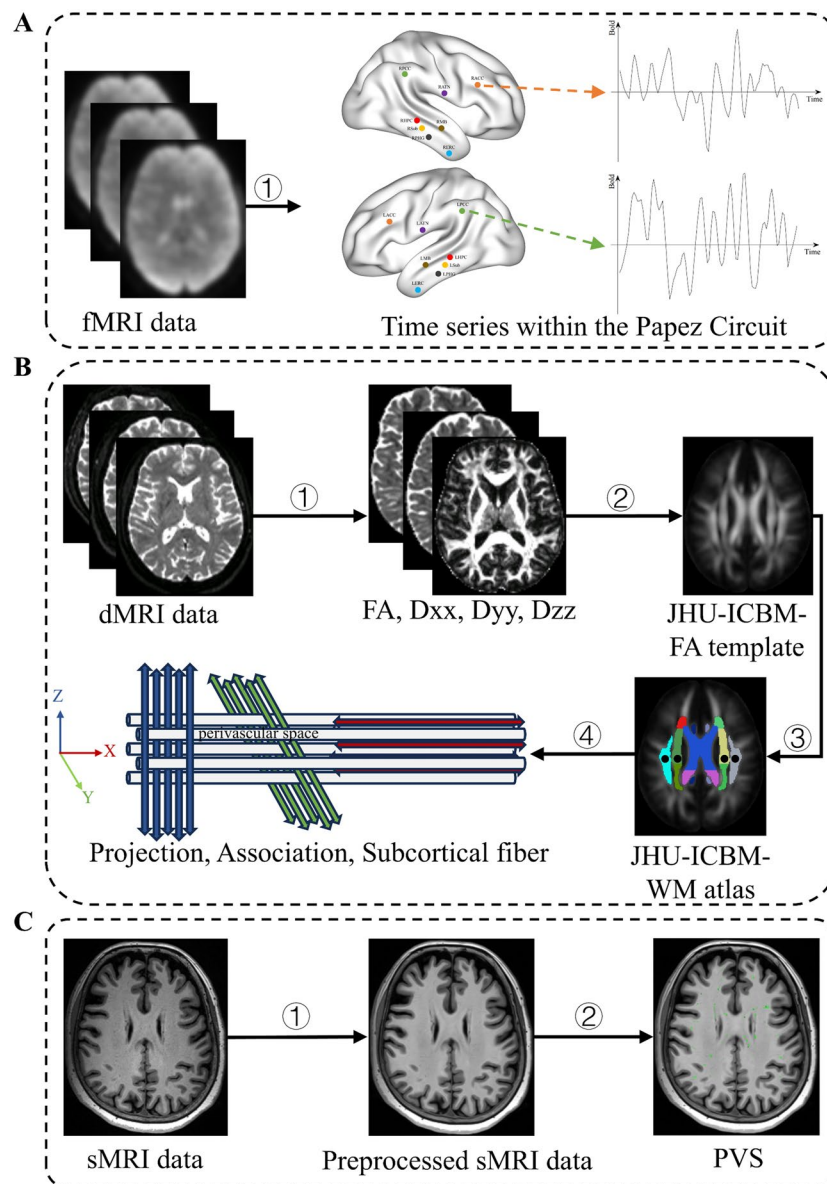


**Fig. 2** Pipelines for data processing. **A** Effective connectivity. ① Extraction of the time series of all brain regions in the Papez circuit. LACC, left anterior cingulate cortex; LATN, left anterior thalamic nuclei; LERC, left entorhinal cortex; LHPC, left hippocampus; LMB, left mamillary body; LPCC, left posterior cingulate cortex; LPHG, left parahippocampal gyrus; LSub, left subiculum; RACC, right anterior cingulate cortex; RATN, right anterior thalamic nuclei; RERC, right entorhinal cortex; RHPC, right hippocampus; RMB, right mamillary body; RPCC, right posterior cingulate cortex; RPHG, right parahippocampal gyrus; RSub, right subiculum. **B** ALPS. ① The dwi2tensor and tensor2metric are used to calculate the tensor metrics of fractional anisotropy (FA) and the diffusivity along the x-axis (right-left; Dxx), y-axis (anterior-posterior; Dyy), and z-axis (inferior-superior; Dzz); ② Register the FA image to the standard space (JHU-ICBM-FA template) and apply the deformation matrix to all diffusivity maps (Dxx, Dyy, Dzz); ③ Place 5 mm diameter spheres on the projection fibers (superior corona radiata (SCR)) and association fibers (superior longitudinal fasciculus (SLF)) at the level of the left and right lateral ventricles; and ④ Obtain the X, Y, and Z directional diffusivity of these fibers. ALPS, along the perivascular space; FA, fractional anisotropy; Dxx, diffusivity along the x-axis (right-left); Dyy, diffusivity along the y-axis (anterior-posterior); Dzz, diffusivity along the z-axis (inferior-superior); JHU-ICBM, Johns Hopkins University - International Consortium for Brain Mapping; WM, white matter. **C** PVS volume. ① T1-weighted images were preprocessed; ② The PVS volume was extracted for quantitative analysis. PVS, perivascular space

**ALPS index**

The calculation of the ALPS index involves the following steps (Fig. 2B): (1) dwi2tensor and tensor2metric are used to calculate the tensor metrics of fractional anisotropy (FA) and the diffusivity along the x-axis (right-left; Dxx),

y-axis (anterior-posterior; Dyy), and z-axis (inferior-superior; Dzz); (2) Register the FA image to the standard space (JHU-ICBM-FA template) and apply the deformation matrix to all diffusivity maps (Dxx, Dyy, Dzz); (3) Place 5 mm diameter spheres on the projection fibers

(superior corona radiata (SCR)) and association fibers (superior longitudinal fasciculus (SLF)) at the level of the left and right lateral ventricles to obtain the X, Y, and Z directional diffusivity of these fibers. According to the JHU-ICBM-DTI-81 white matter labeled atlas, the center coordinates of the ROIs are as follows: left SCR (116, 110, 99), left SLF (128, 110, 99), right SCR (64, 110, 99), and right SLF (51, 110, 99) [44]; (4) The formula for calculating the ALPS index is 
$$\text{ALPS index} = \frac{\text{mean}(D_{xx_{\text{proj}}}, D_{xx_{\text{assoc}}})}{\text{mean}(D_{yy_{\text{proj}}}, D_{zz_{\text{assoc}}})}$$
 [44], where  $D_{xx_{\text{proj}}}$  is the water molecule diffusivity along the x-axis in the projection fiber region;  $D_{xx_{\text{assoc}}}$  is the water molecule diffusivity along the x-axis in the association fiber region;  $D_{yy_{\text{proj}}}$  is the water molecule diffusivity along the y-axis in the projection fiber region; and  $D_{zz_{\text{assoc}}}$  is the water molecule diffusivity along the z-axis in the association fiber region.

### PVS volume

PVS volume analysis includes the following steps (Fig. 2C): (1) T1-weighted images were preprocessed via Advanced Normalization Tools (ANTs, <http://stnava.github.io/ANTs/>, version 2.5.0), which included motion correction, denoising, and nonuniform intensity normalization [45]. Segmentation masks for the basal ganglia (BG) and white matter (WM) were generated via cortical segmentation and reconstructed images from FreeSurfer (<https://surfer.nmr.mgh.harvard.edu/>, version 7.4.1) and FSL. (2) Vessel enhancement was achieved by applying Nonlocal Means (NLM) filtering followed by Frangi vesselness filtering to the T1-weighted images via the Quantitative Imaging Toolkit (QIT, <https://cabeen.io/qitwiki>) [46]. The filtered images were then standardized to normalize vesselness intensities, and a vessel mask was created by applying a threshold to the normalized vesselness map. (3) The PVS volume was extracted from the vessel mask for quantitative analysis. Additionally, the segmentation results were independently reviewed by two senior neuropsychologists, who evaluated the accuracy of the segmentation by assessing the position, shape, and size of the PVS to ensure consistency with the expected anatomical structures.

### Statistical analysis

Statistical analyses of the clinical characteristics were conducted via SPSS version 27.0 software (IBM Corp., Armonk, NY, USA). Intergroup comparisons for continuous variables were performed via a two-sample t test, whereas categorical variables were compared via the  $\chi^2$  test. A two-tailed  $P < 0.05$  was considered statistically significant. The effective connectivity within the Papez circuit, ALPS index, and PVS volume were subjected to group comparisons via a general linear model, with age, sex and education included as covariates. TIV

was included as an additional covariate in the analysis of PVS volume, with the aim of adjusting for inter-individual differences in brain size [47]. For effective connectivity in each hemisphere, the false discovery rate (FDR) was applied to control for multiple comparison errors.

The differential effective connectivity within the Papez circuit, ALPS index, and PVS volume were subjected to linear regression analysis to explore their relationships with neuropsychological test scores, with age, sex, and education as covariates. A two-tailed  $P < 0.05$  was considered statistically significant, and FDR correction was applied for multiple comparisons. The variance inflation factor (VIF) measures the severity of multicollinearity, where a VIF value exceeding 5 generally indicates the presence of multicollinearity [48].

The moderation effects of PVS function on the relationship between differential effective connectivity within the Papez circuit and episodic memory were analyzed via linear regression and Hayes' bootstrap method. Episodic memory impairment, particularly long-delayed recall, was a core symptom of aMCI [49]; therefore, we conducted an exploratory moderation analysis using the AVLT-N5 scores. Furthermore, Hayes' bootstrap method was utilized to generate 5,000 random samples for testing and to calculate the 95% confidence intervals (CI). Moderation analysis was performed via SPSS version 27.0 software (IBM Corp., Armonk, NY, USA), and the significance of the moderation effects was assessed by determining whether the 95% CI excluded zero.

## Results

### Participant characteristics

The clinical characteristics of the participants are summarized in Table 1. The aMCI and HCs groups differed significantly in general cognitive function and memory function ( $P < 0.05$ ) but not in other baseline characteristics, framewise displacement or TIV ( $P > 0.05$ ).

### Effective connectivity and volume within the Papez circuit

After adjusting for age, sex, and education, aMCI patients exhibited significant reductions in effective connectivity from the left MB to the left ACC, left ATN and left PHG; from the left PCC to the left ACC and left HPC; from the left PHG to the left ERC and left PHG; and from the left Sub to the left PHG and left Sub compared with HCs ( $P < 0.05$ , FDR corrected) (Fig. 3). Similarly, aMCI patients exhibited significant reductions in effective connectivity from the right ACC to the right HPC, from the right HPC to the right ATN, from the right PHG to the right ATN, and from the right Sub to the right ACC compared with HCs ( $P < 0.05$ , FDR corrected) (Fig. 4). However, no differences were observed in the Papez circuit volume between aMCI patients and HCs ( $P > 0.05$ ) (Table 1). After adjusting for age, sex, and education,

**Table 1** Clinical characteristics and neuropsychological test results

Characteristics	HCs	aMCI	T/ $\chi^2$	P
N	32	28	-	-
Age (y), mean (SD)	64.63 (6.56)	67.14 (7.24)	-1.413	0.163
Education (y), mean (SD)	11.78 (3.05)	11.61 (3.10)	0.219	0.827
Female, N (%)	25 (78.13)	16 (57.14)	3.038	0.081
Smoke, N (%)	4 (12.50)	6 (21.43)	0.857	0.355
Drink, N (%)	5 (15.63)	4 (14.29)	0.021	0.885
Height (cm), mean (SD)	163.77 (6.06)	160.92 (12.64)	1.031	0.310
Weight (kg), mean (SD)	62.04 (9.92)	62.68 (12.48)	-0.211	0.833
FD <sub>Jenkinson</sub>	0.067 (0.026)	0.081 (0.033)	-0.013	0.093
FD <sub>Power</sub>	0.118 (0.036)	0.132 (0.034)	-0.014	0.141
MMSE, mean (SD)	28.47 (1.50)	27.25 (1.58)	3.062	0.003
MoCA-B, mean (SD)	26.44 (1.90)	22.46 (3.00)	6.208	<0.001
AVLT, mean (SD)	60.53 (8.70)	35.61 (4.91)	13.882	<0.001
AVLT-N1, mean (SD)	4.09 (1.30)	2.96 (0.92)	3.821	<0.001
AVLT-N2, mean (SD)	6.84 (1.61)	4.46 (0.96)	7.051	<0.001
AVLT-N3, mean (SD)	8.28 (1.46)	5.25 (1.27)	8.517	<0.001
AVLT-N4, mean (SD)	6.69 (1.62)	2.36 (1.31)	11.295	<0.001
AVLT-N5, mean (SD)	6.28 (1.75)	1.54 (1.29)	11.828	<0.001
AVLT-N6, mean (SD)	6.09 (2.36)	1.89 (1.34)	8.602	<0.001
AVLT-N7, mean (SD)	22.25 (1.44)	17.14 (1.78)	12.296	<0.001
FAQ, mean (SD)	0.22 (0.91)	0.96 (1.71)	-2.067	0.045
TIV (cm <sup>3</sup> ), mean (SD)	1388.66 (117.86)	1434.02 (124.18)	-1.451	0.152
LACC (cm <sup>3</sup> ), mean (SD)	0.36 ± 0.04	0.35 ± 0.04	0.693	0.491
LATN (cm <sup>3</sup> ), mean (SD)	0.26 ± 0.03	0.25 ± 0.03	0.452	0.653
LERC (cm <sup>3</sup> ), mean (SD)	0.47 ± 0.06	0.47 ± 0.08	0.357	0.722
LHPC (cm <sup>3</sup> ), mean (SD)	0.41 ± 0.04	0.39 ± 0.06	1.463	0.150
LMB (cm <sup>3</sup> ), mean (SD)	0.14 ± 0.02	0.14 ± 0.01	0.216	0.830
LPCC (cm <sup>3</sup> ), mean (SD)	0.36 ± 0.06	0.35 ± 0.05	0.523	0.603
LPHG (cm <sup>3</sup> ), mean (SD)	0.39 ± 0.03	0.39 ± 0.04	0.745	0.459
LSub (cm <sup>3</sup> ), mean (SD)	0.47 ± 0.05	0.45 ± 0.07	1.706	0.093
RACC (cm <sup>3</sup> ), mean (SD)	0.28 ± 0.03	0.27 ± 0.03	1.543	0.128
RATN (cm <sup>3</sup> ), mean (SD)	0.25 ± 0.02	0.25 ± 0.03	0.519	0.606
RERC (cm <sup>3</sup> ), mean (SD)	0.42 ± 0.06	0.42 ± 0.07	-0.027	0.979
RHPC (cm <sup>3</sup> ), mean (SD)	0.39 ± 0.04	0.37 ± 0.05	1.377	0.174
RMB (cm <sup>3</sup> ), mean (SD)	0.14 ± 0.02	0.14 ± 0.01	0.355	0.724
RPCC (cm <sup>3</sup> ), mean (SD)	0.27 ± 0.04	0.26 ± 0.04	0.491	0.625
RPHG (cm <sup>3</sup> ), mean (SD)	0.44 ± 0.04	0.44 ± 0.05	0.659	0.512
RSub (cm <sup>3</sup> ), mean (SD)	0.49 ± 0.06	0.47 ± 0.06	1.445	0.154
Left hippocampal volume supplied by the choroidal artery	0.60 ± 0.07	0.56 ± 0.10	1.606	0.114
Left hippocampal volume supplied by the hippocampal artery	2.82 ± 0.32	2.69 ± 0.41	1.324	0.191

**Table 1** (continued)

Characteristics	HCs	aMCI	T/ $\chi^2$	P
Right hippocampal volume supplied by the choroidal artery	0.62 ± 0.07	0.60 ± 0.07	1.045	0.301
Right hippocampal volume supplied by the hippocampal artery	9.82 ± 1.09	9.44 ± 1.28	1.243	0.219

aMCI, amnesic mild cognitive impairment; HCs, healthy controls; BMI, body mass index; MMSE, Mini-Mental State Examination; MoCA-B, Montreal Cognitive Assessment-Basic; AVLT, Auditory Verbal Learning Test; AVLT-N1, Auditory Verbal Learning Test, First Immediate Recall; AVLT-N2, Auditory Verbal Learning Test, Second Immediate Recall; AVLT-N3, Auditory Verbal Learning Test, the Third Immediate Recall; AVLT-N4, Auditory Verbal Learning Test, Short-Term Delay Recall; AVLT-N5, Auditory Verbal Learning Test, Long-Term Delay Recall; AVLT-N6, Auditory Verbal Learning Test, Long Delay Cued Recall; AVLT-N7, Auditory Verbal Learning Test, Recognition; FAQ, Functional Activities Questionnaire; TIV, total intracranial volume; FD, framewise displacement

linear regression analysis revealed several significant associations (Supplementary Table S3). The effective connectivity from the left PCC to the left HPC and from the left Sub to the left Sub was significantly associated with the MoCA-B score ( $\beta = 0.319$ ,  $P < 0.05$ , FDR correction;  $\beta = 0.383$ ,  $P < 0.05$ , FDR correction). The effective connectivity from the left PCC to the left HPC and from the right Sub to the right ACC was significantly associated with the FAQ score ( $\beta = -0.223$ ,  $P < 0.05$ , FDR correction;  $\beta = -0.308$ ,  $P < 0.05$ , FDR correction). Additionally, the effective connectivity from the left Sub to the left PHG was significantly associated with the AVLT-N7 score ( $\beta = 0.290$ ,  $P < 0.05$ , FDR correction). The effective connectivity from the left PHG to the left ERC was significantly associated with the AVLT-N5 score ( $\beta = 0.323$ ,  $P < 0.001$ , FDR correction) and AVLT-N3 score ( $\beta = 0.422$ ,  $P < 0.05$ , FDR correction).

**PVS function**

After adjusting for age, sex, and education, significant reductions in the ALPS index were observed in aMCI patients compared with HCs ( $P < 0.001$ ) (Fig. 5A). Similarly, after adjusting for age, sex, education, and TIV, the PVS volume was significantly greater in aMCI patients than in HCs ( $P < 0.001$ ) (Fig. 5B). The ALPS index was significantly associated with the MMSE score ( $\beta = 0.261$ ,  $P < 0.05$ , FDR correction) and AVLT score ( $\beta = 0.237$ ,  $P < 0.05$ , FDR correction). Additionally, the PVS volume was significantly associated with the AVLT score ( $\beta = -0.479$ ,  $P < 0.001$ , FDR correction), AVLT-N2 score ( $\beta = -0.427$ ,  $P < 0.05$ , FDR correction), AVLT-N4 score ( $\beta = -0.443$ ,  $P < 0.05$ , FDR correction), AVLT-N5 score ( $\beta = -0.460$ ,  $P < 0.001$ , FDR correction), AVLT-N7 score ( $\beta = -0.467$ ,  $P < 0.001$ , FDR correction) and FAQ score ( $\beta = 0.477$ ,  $P < 0.001$ , FDR correction) (Supplementary Table S3).

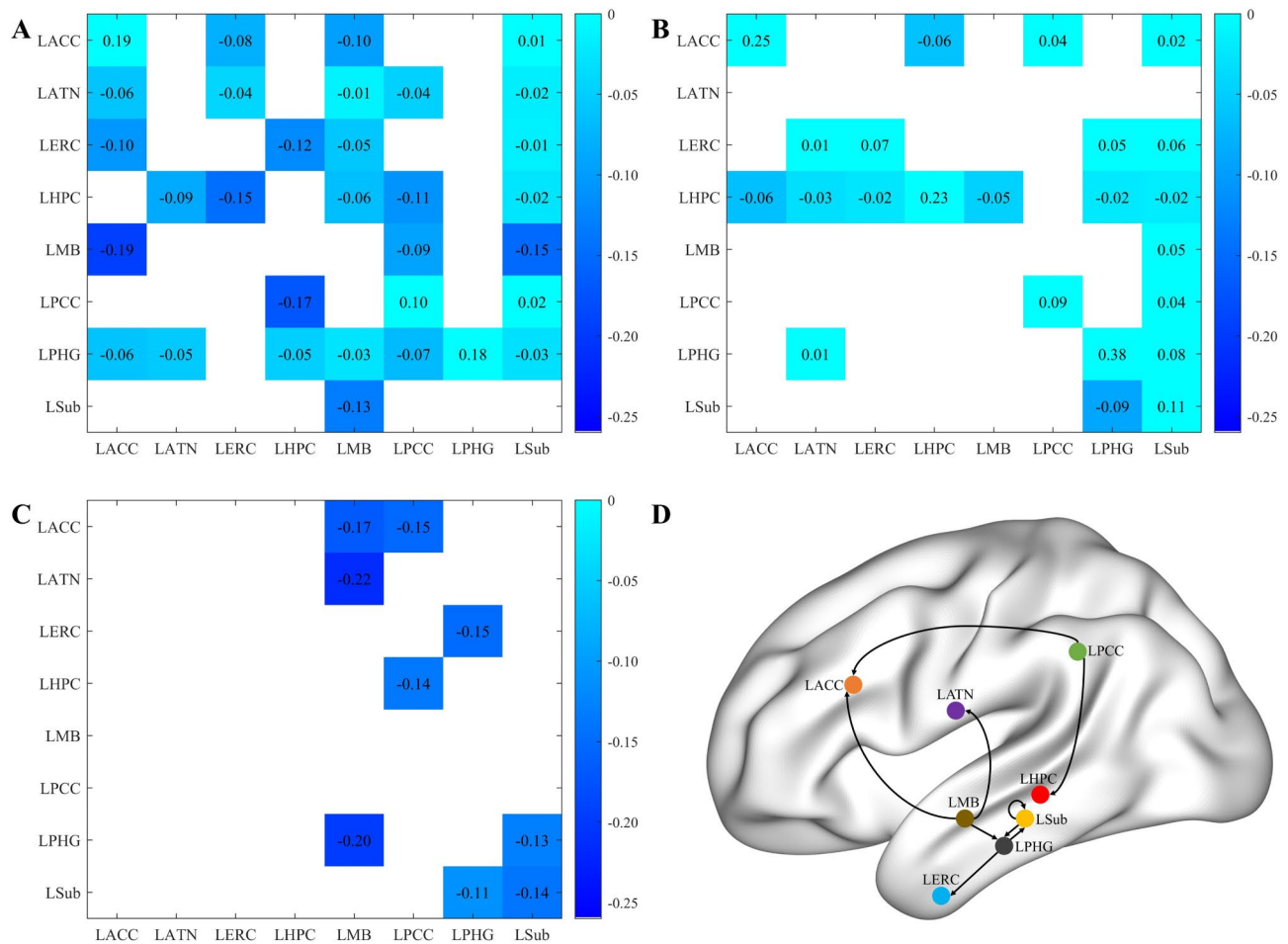


**Fig. 3** Results of the left effective connectivity. **A** The left effective connectivity significantly different from zero in aMCI patients. **B** The left effective connectivity significantly differed from zero in HCs. **C** Group differences in the left effective connectivity. aMCI, amnesic mild cognitive impairment; HCs, healthy controls; LACC, left anterior cingulate cortex; LATN, left anterior thalamic nuclei; LERC, left entorhinal cortex; LHPC, left hippocampus; LMB, left mamillary body; LPCC, left posterior cingulate cortex; LPHG, left parahippocampal gyrus; LSub, left subiculum

**Moderation analysis**

Moderation analysis revealed that the ALPS index moderated the relationships between the effective connectivity from the right HPC to the right ATN and the AVLT-N5 score ( $\beta = -0.319, P = 0.014$ ) (Fig. 6).

**Discussion**

This study systematically explored the relationships among effective connectivity within the Papez circuit, PVS function, and episodic memory. The findings demonstrated that the effective connectivity between multiple critical regions within the Papez circuit, notably in the hippocampus, anterior cingulate cortex, and parahippocampal gyrus, was significantly weakened in aMCI patients. Moreover, a significant reduction in the ALPS index was observed among aMCI patients, accompanied by a marked increase in PVS volume, indicating significant PVS dysfunction. Further moderation analysis revealed that PVS function moderated the relationship

between effective connectivity within the Papez circuit and episodic memory impairment, emphasizing the critical role of PVS function in mitigating the impact of effective connectivity within the Papez circuit on episodic memory.

The weakening of effective connectivity within the Papez circuit is a crucial factor contributing to the decline in episodic memory in aMCI patients. As the connectivity among key regions, including the HPC, ACC, and PHG within the Papez circuit, weakens, there is a marked reduction in neural transmission efficiency, which subsequently impacts episodic memory processes such as encoding, consolidation, and retrieval. Under normal conditions, the effective connections between these brain regions help maintain synaptic plasticity and long-term potentiation (LTP) [50], thereby ensuring efficient communication between different brain regions. LTP is the foundation of episodic memory encoding and consolidation, and when the effective connections within the Papez

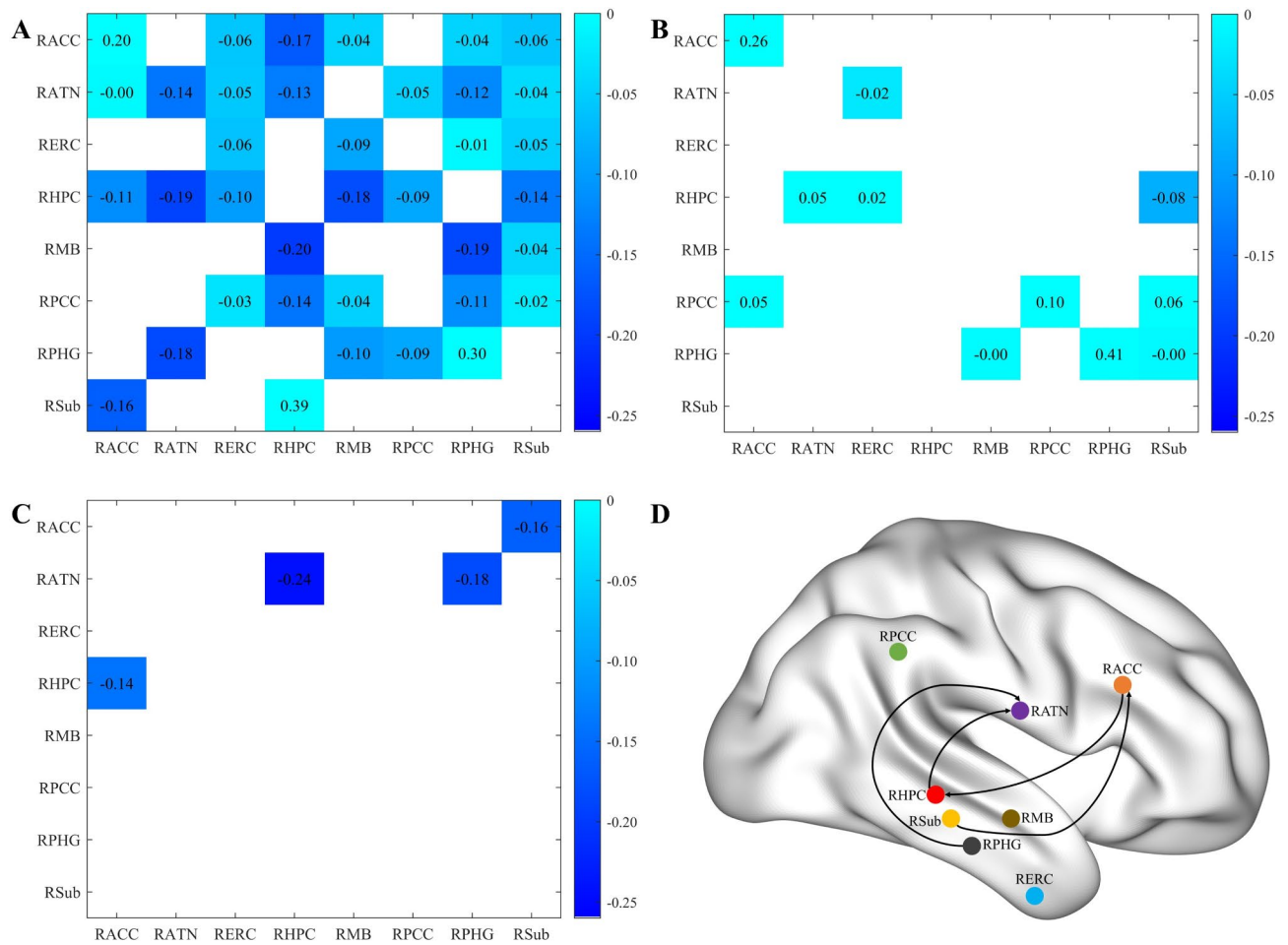


**Fig. 4** Results of the right effective connectivity. **A** The right effective connectivity significantly different from zero in aMCI patients. **B** The right effective connectivity significantly differed from zero in HCs. **C** Group differences in the right effective connectivity. aMCI, amnesic mild cognitive impairment; HCs, healthy controls; RACC, right anterior cingulate cortex; RATN, right anterior thalamic nuclei; RERC, right entorhinal cortex; RHPC, right hippocampus; RMB, right mamillary body; RPCC, right posterior cingulate cortex; RPHG, right parahippocampal gyrus; RSub, right subiculum

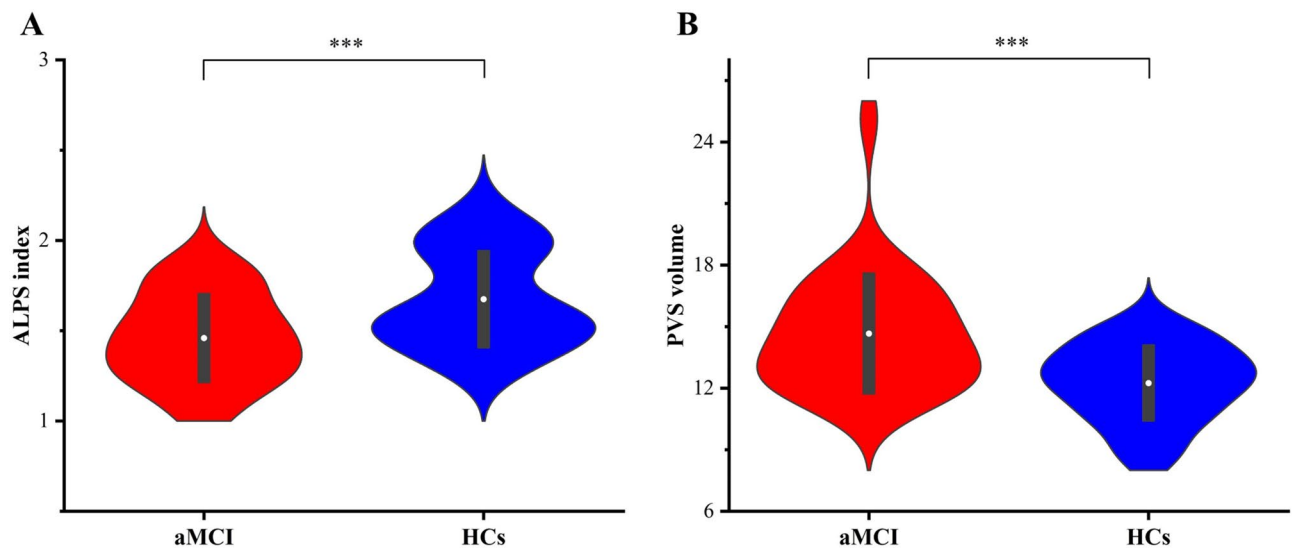


**Fig. 5** Group differences in the ALPS index and PVS volume. **A** ALPS index. **B** PVS volume. aMCI, amnesic mild cognitive impairment; HCs, healthy controls; ALPS, along the perivascular space; PVS, perivascular space; \*,  $P < 0.05$ ; \*\*,  $P < 0.01$ ; \*\*\*,  $P < 0.001$ ; ns,  $P > 0.05$

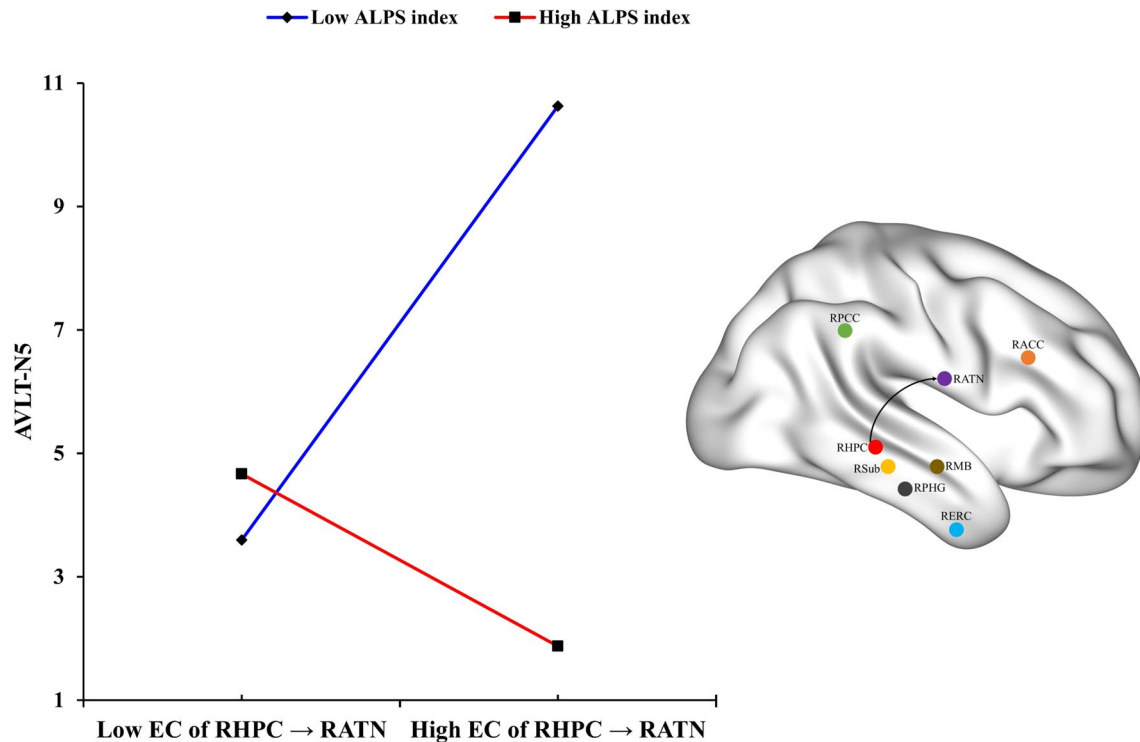


**Fig. 6** Moderation analysis results. EC, effective connectivity; RATN, right anterior thalamic nuclei; RHPC, right hippocampus; AVLT-N5, Auditory Verbal Learning Test, Long-Term Delay Recall; ALPS, along the perivascular space \*,  $P < 0.05$ ; \*\*,  $P < 0.01$ ; \*\*\*,  $P < 0.001$ ; ns,  $P > 0.05$

circuit are damaged, maintaining LTP becomes challenging, thus hindering the integration of new information and the formation of long-term memory [51]. In aMCI patients, the significant weakening of effective connections, particularly between the left LMB, ACC, ATN, and PHG and between the right HPC, ACC, and ATN, may reflect a greater degree of impaired neural network integration. This integrative impairment not only restricts the central role of the HPC in episodic memory but also may lead to dysregulation in the interaction between other brain networks, such as the default mode network and the Papez circuit, further exacerbating cognitive decline. Research by Avesis supports this view, indicating that key overlapping regions between the Papez circuit and the default mode network, such as the connection between the ventral cingulate gyrus and the HPG, may play a crucial role in the early impairment of episodic memory [52]. These findings suggest that the effective connections within the Papez circuit are not only crucial for independent episodic memory processing but also play a key role in maintaining overall cognitive function via their collaboration with other brain networks [53]. Importantly, the findings raise the question of causality: does weakened connectivity within the Papez circuit lead to PVS dysfunction, or does PVS dysfunction lead to weakened connectivity? PVS dysfunction could contribute to weakened connectivity within the Papez circuit by impairing the clearance of neurotoxic proteins, which disrupts synaptic

function and neural network efficiency [15, 54, 55]. Conversely, it is also possible that weakened connectivity and disrupted neural activity within the Papez circuit could contribute to PVS dysfunction by impairing metabolic regulation and cerebrospinal fluid flow [56]. The dynamic and potentially reciprocal relationships among these factors highlight the need for future longitudinal studies to disentangle the temporal sequence and directionality of these changes.

PVS dysfunction may impact the formation and maintenance of episodic memory through various complex neurobiological mechanisms. PVS dysfunction primarily manifests as reduced clearance of metabolic waste, particularly regarding the accumulation of toxic proteins [15, 55]. The accumulation of these toxic proteins not only impairs synaptic transmission but also triggers neuro-inflammatory cascades, resulting in the exacerbation of neuronal damage and the progression of degeneration. As metabolic waste accumulates, oxidative stress and microglial activation are triggered, resulting in the release of substantial amounts of inflammatory mediators [54]. These inflammatory mediators not only compromise the integrity of the blood–brain barrier but also impair memory processes, including encoding, consolidation, and retrieval, by disrupting brain structure and function, particularly synaptic plasticity and LTP in regions involved in episodic memory, such as the HPC and PHG [57–59]. As the central structure of episodic memory, the normal

function of the HPC depends on stable neuronal connections and minimal neuroinflammation to sustain the processing and storage of new information [59]. However, when the PVS fails to efficiently clear toxic metabolic byproducts, the metabolic burden on neurons significantly increases, leading to impaired synaptic transmission and structural plasticity in the HPC, eventually resulting in a gradual decline in episodic memory. Therefore, PVS dysfunction not only accelerates neurodegenerative processes but also triggers widespread metabolic imbalances, blood-brain barrier disruption, and global inflammatory responses, leading to widespread disruption of neuronal connectivity networks. In other words, the decline in episodic memory in aMCI patients is not solely attributable to neurodegenerative pathology but also reflects more complex neurobiological mechanisms, such as metabolic imbalances in the brain and impaired synaptic function.

The results of the regression analysis indicated that the differential effective connectivity within the Papez circuit and PVS function is significantly associated with cognitive function, especially episodic memory. Moderation analysis revealed that PVS function modulates the relationship between the effective connectivity within the Papez circuit and episodic memory. PVS mitigates the adverse effects of weakened connectivity within the Papez circuit on episodic memory by clearing metabolic waste from the brain and reducing neuronal damage resulting from neuroinflammation and oxidative stress. Therefore, even if the effective connectivity within the Papez circuit is weakened, proper functioning of the PVS can partly compensate for this deficit, thus mitigating cognitive decline. Du and colleagues demonstrated that the local application of prostaglandin F<sub>2α</sub> can increase the clearance capacity of the central nervous system, providing a promising approach for enhancing PVS function [60]. On the basis of these findings, future intervention strategies should emphasize both the enhancement of connectivity within the Papez circuit and the improvement of PVS function, particularly in the early stages of aMCI.

### Limitations

While this study elucidates the intricate relationships among PVS function, the Papez circuit, and episodic memory, several limitations must be considered. First, the study's sample size is limited, and future studies should seek to increase the sample size and be conducted across multiple centers to improve the external validity and generalizability of the findings. Second, the inclusion criteria for aMCI patients in this study did not include biomarker confirmation (e.g., amyloid status), which limits the ability to distinguish Alzheimer's-related aMCI from other potential etiologies. Future studies should

include biomarker-based assessments to refine diagnostic specificity and achieve a more precise understanding of Alzheimer's disease-related mechanisms. Third, although DTI-ALPS and PVS volume serve as imaging markers of PVS function, these techniques have inherent limitations in accurately characterizing perivascular dynamics and glymphatic clearance, as the ALPS index may be affected by axonal damage or microstructural alterations in white matter. Additionally, although this study uncovers the intricate interplay between PVS function and the Papez circuit, future longitudinal studies will be essential for monitoring their dynamic changes and interaction patterns over time. Finally, this study focused on the Papez circuit, and future research should explore additional neural systems, such as the default mode network and the prefrontal-hippocampal network, to better elucidate the neural mechanisms of memory decline and their roles in early cognitive impairment.

### Conclusion

In conclusion, this study demonstrated the relationships between PVS function, effective connectivity within the Papez circuit, and episodic memory and that PVS function can moderate the relationship between effective connectivity within the Papez circuit and episodic memory. In other words, enhancing PVS function may mitigate the adverse effects of weakened effective connectivity in the Papez circuit on episodic memory in aMCI patients. Improving PVS function may serve as a promising therapeutic target for protecting against cognitive decline and could foster breakthroughs in the treatment of aMCI.

### Supplementary Information

The online version contains supplementary material available at <https://doi.org/10.1186/s13195-025-01717-7>.

Supplementary Material 1

Supplementary Material 2

### Acknowledgements

The authors thank all the participants who participated in this study.

### Author contributions

Ling-Ling Li (Writing-original draft, Methodology), Jie Ma (Methodology, Project administration, Writing-review & editing), Jia-Jia Wu (Methodology, Project administration, Writing-review & editing), Xin Xue (Formal Analysis, Investigation, Methodology), Mou-Xiong Zheng (Conceptualization, Funding acquisition, Project administration, Supervision), Xu-Yun Hua (Conceptualization, Funding acquisition, Project administration, Supervision), Qi-Hao Guo (Conceptualization, Funding acquisition, Project administration, Supervision), and Jian-Guang Xu (Conceptualization, Funding acquisition, Project administration, Supervision). All the authors contributed to the article and approved the submitted version.

### Funding

This work was supported by the National Key R&D Program of China (Grant Nos. 2018YFC2001600 and 2018YFC2001604); National Natural Science Foundation of China (Grant Nos. 82272583, 82172554, 82272589, 81871836, 82302870 and 81902301); Shanghai Health Care Commission (Grant No.

2022JC026); Shanghai Science and Technology Committee (Grant No. 22010504200); Shanghai Rising-Star Program (Grant No. 23QA1409200); Shanghai Youth Top Talent Development Plan; Shanghai "Rising Stars of Medical Talent" - Distinguished Young Medical Talent Program; Shanghai Talent Development Fund (2021074), Science & Technology Development Fund of Shanghai University of Traditional Chinese Medicine (Grant No. 23KFL112); High-level Chinese Medicine Key Discipline Construction Project (Integrative Chinese and Western Medicine Clinic) of National Administration of TCM (zyzdxk-2023065); and Shanghai Hospital Development Center Foundation-Shanghai Municipal Hospital Rehabilitation Medicine Specialty Alliance (SHDC22023304).

#### Data availability

No datasets were generated or analysed during the current study.

#### Declarations

#### Ethics approval and consent to participate

Approval for the study was obtained from the ethics committee of Shanghai Jiao Tong University Affiliated Sixth People's Hospital (NO. 2019-041), in accordance with the Declaration of Helsinki, and all participants provided informed consent.

#### Competing interests

The authors declare no competing interests.

#### Author details

<sup>1</sup>Department of Rehabilitation Medicine, Yueyang Hospital of Integrated Traditional Chinese and Western Medicine, Shanghai University of Traditional Chinese Medicine, Shanghai 200437, China

<sup>2</sup>School of Rehabilitation Science, Shanghai University of Traditional Chinese Medicine, Shanghai 201203, China

<sup>3</sup>Department of Traumatology and Orthopedics, Shuguang Hospital, Shanghai University of Traditional Chinese Medicine, Shanghai 201203, China

<sup>4</sup>Department of Gerontology, Shanghai Sixth People's Hospital, Shanghai Jiao Tong University School of Medicine, Shanghai 200233, China

<sup>5</sup>Engineering Research Center of Traditional Chinese Medicine Intelligent Rehabilitation, Ministry of Education, Shanghai 201203, China

Received: 13 October 2024 / Accepted: 13 March 2025

Published online: 21 March 2025

#### References

- Petersen RC. Clinical practice. Mild cognitive impairment. *N Engl J Med*. 2011;364(23):2227–34.
- Gauthier S, et al. Mild cognitive impairment. *Lancet*. 2006;367(9518):1262–70.
- Chatzikostopoulos A, et al. Episodic memory in amnesic mild cognitive impairment (aMCI) and Alzheimer's disease dementia (ADD): using the doors and people tool to differentiate between early aMCI-late aMCI-mild add diagnostic groups. *Diagnostics (Basel)*. 2022;12(7):1768.
- Escobar I, et al. Altered neural networks in the Papez circuit: implications for cognitive dysfunction after cerebral ischemia. *J Alzheimers Dis*. 2019;67(2):425–46.
- Rapaka D, et al. Targeting Papez circuit for cognitive dysfunction- insights into deep brain stimulation for Alzheimer's disease. *Heliyon*. 2024;10(9):e30574.
- Moscovitch M, et al. Episodic memory and beyond: the hippocampus and neocortex in transformation. *Annu Rev Psychol*. 2016;67:105–34.
- Chu CS, et al. Cognitive effects and acceptability of non-invasive brain stimulation on Alzheimer's disease and mild cognitive impairment: A component network meta-analysis. *J Neurol Neurosurg Psychiatry*. 2021;92(2):195–203.
- Chou YH, et al. Cortical excitability and plasticity in Alzheimer's disease and mild cognitive impairment: A systematic review and meta-analysis of transcranial magnetic stimulation studies. *Ageing Res Rev*. 2022;79:101660.
- López-Alonso V, et al. Inter-individual variability in response to non-invasive brain stimulation paradigms. *Brain Stimul*. 2014;7(3):372–80.
- Freitas C, et al. Noninvasive brain stimulation in Alzheimer's disease: systematic review and perspectives for the future. *Exp Gerontol*. 2011;46(8):611–27.
- Cai Y, et al. The relationship between inflammation, impaired glymphatic system, and neurodegenerative disorders: A vicious cycle. *Neurobiol Dis*. 2024;192:106426.
- Tuovinen T, et al. The variability of functional MRI brain signal increases in Alzheimer's disease at cardiorespiratory frequencies. *Sci Rep*. 2020;10(1):21559.
- Rajna Z, et al. 3D multi-resolution optical flow analysis of cardiovascular pulse propagation in human brain. *IEEE Trans Med Imaging*. 2019;38(9):2028–36.
- Peters ME, et al. The glymphatic system's role in traumatic brain injury-related neurodegeneration. *Mol Psychiatry*. 2023;28(7):2707–15.
- Rajna Z, et al. Cardiovascular brain impulses in Alzheimer's disease. *Brain*. 2021;144(7):2214–26.
- Kiviniemi V, et al. Ultra-fast magnetic resonance encephalography of physiological brain activity-Glymphatic pulsation mechanisms? *J Cereb Blood Flow Metab*. 2016;36(6):1033–45.
- Turamanlar O, et al. Perivascular (Virchow–Robin) spaces. *Kastamonu Med J*. 2021;1:85–8.
- Liu X, et al. MRI free water mediates the association between diffusion tensor image analysis along the perivascular space and executive function in four independent middle to aged cohorts. *Alzheimers Dement*. 2025;21(2):e14453.
- Khawaja AZ, et al. Revisiting the risks of MRI with gadolinium based contrast agents-review of literature and guidelines. *Insights into Imaging*. 2015;6(5):553–8.
- Pasquini L, et al. Gadolinium-based contrast agent-related toxicities. *CNS Drugs*. 2018;32(3):229–40.
- Taoka T, et al. Evaluation of glymphatic system activity with the diffusion MR technique: diffusion tensor image analysis along the perivascular space (DTI-ALPS) in Alzheimer's disease cases. *Jpn J Radiol*. 2017;35(4):172–8.
- Taoka T, et al. Reproducibility of diffusion tensor image analysis along the perivascular space (DTI-ALPS) for evaluating interstitial fluid diffusivity and glymphatic function: changes in alps index on multiple condition acquisition experiment (chamonix) study. *Jpn J Radiol*. 2022;40(2):147–58.
- Zhang J, et al. Enlarged perivascular space and index for diffusivity along the perivascular space as emerging neuroimaging biomarkers of neurological diseases. *Cell Mol Neurobiol*. 2023;44(1):14.
- Iliff JJ, et al. A paravascular pathway facilitates CSF flow through the brain parenchyma and the clearance of interstitial solutes, including amyloid B. *Sci Transl Med*. 2012;4(147):147ra11.
- Bondi MW, et al. Neuropsychological criteria for mild cognitive impairment improves diagnostic precision, biomarker associations, and progression rates. *J Alzheimers Dis*. 2014;42(1):275–89.
- Arevalo-Rodríguez I, et al. Mini-Mental state examination (MMSE) for the early detection of dementia in people with mild cognitive impairment (MCI). *Cochrane Database Syst Rev*. 2021;7(7):Cd010783.
- Ma J, et al. Mapping the long-term delayed recall-based cortex-hippocampus network constrained by the structural and functional connectome: A case-control multimodal MRI study. *Alzheimers Res Ther*. 2023;15(1):61.
- González DA, et al. Comprehensive evaluation of the functional activities questionnaire (FAQ) and its reliability and validity. *Assessment*. 2021;29(4):748–63.
- Morris JC. The clinical dementia rating (CDR): current version and scoring rules. *Neurology*. 1993;43(11):2412–4.
- McKhann GM, et al. The diagnosis of dementia due to Alzheimer's disease: recommendations from the National Institute on Aging-Alzheimer's association workgroups on diagnostic guidelines for Alzheimer's disease. *Alzheimers Dement*. 2011;7(3):263–9.
- Chen KL, et al. Validation of the Chinese version of Montreal cognitive assessment basic for screening mild cognitive impairment. *J Am Geriatr Soc*. 2016;64(12):e285–90.
- Chen H, et al. The characteristic patterns of individual brain susceptibility networks underlie Alzheimer's disease and white matter hyperintensity-related cognitive impairment. *Transl Psychiatry*. 2024;14(1):177.
- Silva PHR, et al. Brain functional and effective connectivity underlying the information processing speed assessed by the symbol digit modalities test. *NeuroImage*. 2019;184:761–70.
- Knesevich JW, et al. Predictive value of the Boston naming test in mild senile dementia of the alzheimer type. *Psychiatry Res*. 1986;19(2):155–61.
- Chen NC, et al. Patterns of executive dysfunction in amnesic mild cognitive impairment. *Int Psychogeriatr*. 2013;25(7):1181–9.

36. Akkoyun M, et al. Eye movements during the judgment of line orientation test in patients with Alzheimer's disease and amnesic mild cognitive impairment. *Alzheimers Dement*. 2023;19:e075697.
37. Pruim RHR, et al. ICA-AROMA: A robust ICA-based strategy for removing motion artifacts from fMRI data. *NeuroImage*. 2015;112:267–77.
38. Satterthwaite TD, et al. An improved framework for confound regression and filtering for control of motion artifact in the preprocessing of resting-state functional connectivity data. *NeuroImage*. 2013;64:240–56.
39. Weiler M, et al. Evaluating denoising strategies in resting-state functional magnetic resonance in traumatic brain injury (EpiBioS4Rx). *Hum Brain Mapp*. 2022;43(15):4640–9.
40. Tournier JD, et al. MRtrix3: A fast, flexible and open software framework for medical image processing and visualisation. *NeuroImage*. 2019;202:116137.
41. Marchesi O, et al. Resting state effective connectivity abnormalities of the Papez circuit and cognitive performance in multiple sclerosis. *Mol Psychiatry*. 2022;27(9):3913–9.
42. Razi A, et al. Construct validation of a DCM for resting state fMRI. *NeuroImage*. 2015;106:1–14.
43. Friston KJ, et al. A DCM for resting state fMRI. *NeuroImage*. 2014;94(100):396–407.
44. Liu X, et al. Cross-vendor test-retest validation of diffusion tensor image analysis along the perivascular space (DTI-ALPS) for evaluating glymphatic system function. *Aging Dis*. 2023;15(4):1885–98.
45. Kamagata K, et al. Association of MRI indices of glymphatic system with amyloid deposition and cognition in mild cognitive impairment and alzheimer disease. *Neurology*. 2022;99(24):e2648–60.
46. Amjadi M, et al. Enhancing vascular network visualization in 3D photoacoustic imaging: in vivo experiments with a vasculature filter. *Opt Express*. 2024;32(15):25533–44.
47. Malone IB, et al. Accurate automatic Estimation of total intracranial volume: A nuisance variable with less nuisance. *NeuroImage*. 2015;104:366–72.
48. Kim JH. Multicollinearity and misleading statistical results. *Korean J Anesthesiol*. 2019;72(6):558–69.
49. Wearn AR, et al. Accelerated long-term forgetting in healthy older adults predicts cognitive decline over 1 year. *Alzheimers Res Ther*. 2020;12(1):119.
50. Bliss TV, et al. A synaptic model of memory: Long-term potentiation in the hippocampus. *Nature*. 1993;361(6407):31–9.
51. Aggleton JP, et al. Time to retire the serial Papez circuit: implications for space, memory, and attention. *Neurosci Biobehav Rev*. 2022;140:104813.
52. Hari E, et al. Functional and structural connectivity in the Papez circuit in different stages of Alzheimer's disease. *Clin Neurophysiol*. 2023;153:33–45.
53. Hall S. Is the Papez circuit the location of the elusive episodic memory engram? *IBRO Neurosci Rep*. 2024;16:249–59.
54. Gu S, et al. Glymphatic dysfunction induced oxidative stress and neuro-inflammation in major depression disorders. *Antioxid (Basel)*. 2022;11(11):2296.
55. Rabbito A et al. Biochemical markers in Alzheimer's disease. *Int J Mol Sci*. 2020; 21(6): 1989.
56. Xavier J, et al. Intriguing role of gut-brain axis on cognition with an emphasis on interaction with Papez circuit. *CNS Neurol Disord Drug Targets*. 2023;22(8):1146–63.
57. Hablitz LM, et al. The glymphatic system: A novel component of fundamental neurobiology. *J Neurosci*. 2021;41(37):7698–711.
58. Sun Y, et al. Association study of brain structure–function coupling and glymphatic system function in patients with mild cognitive impairment due to Alzheimer's disease. *Front Neurosci*. 2024;18:1417986.
59. Mancini A, et al. Hippocampal neuroplasticity and inflammation: relevance for multiple sclerosis. *Mult Scler Demyelinating Disord*. 2017;2:1–12.
60. Du T, et al. Restoration of cervical lymphatic vessel function in aging rescues cerebrospinal fluid drainage. *Nat Aging*. 2024;4(10):1418–31.

#### Publisher's note

Springer Nature remains neutral with regard to jurisdictional claims in published maps and institutional affiliations.